FERMILAB-SLIDES-24-0264-PPD

(Work supported by DOE)

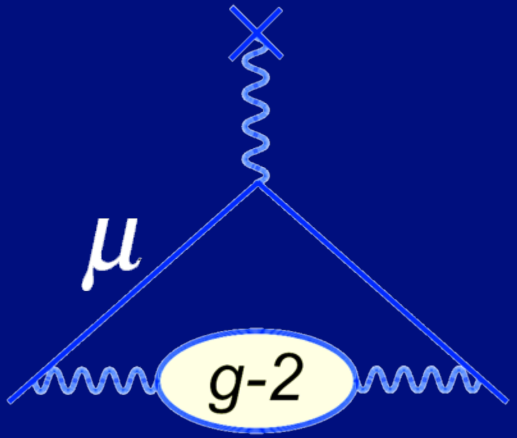

Beam Dynamics of the Muon g-2 Experiment

Eremey Valetov

Michigan State University

On behalf of the Muon g−2 Collaboration

MICHIGAN STATE UNIVERSITY

U.S. DEPARTMENT OF ENERGY | Office of Science

ICAP 2024, Seeheim, Germany – October 4th, 2024

$\mu = g \frac{e}{2m} s$ Gyromagnetic ratio equation

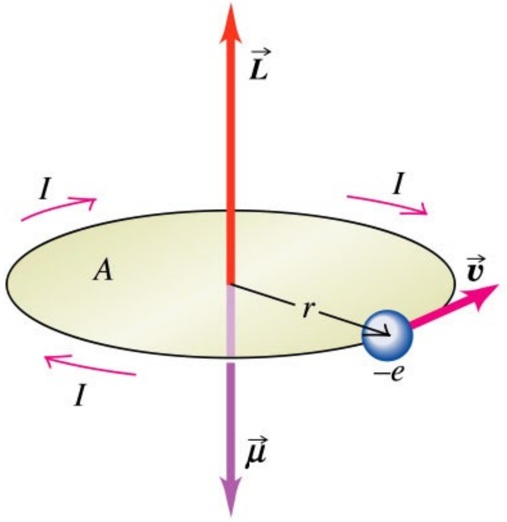

Classical: $g = 1$

Dirac Equation: $g = 2$

$i\left(\partial_\mu - ieA_\mu(x)\right)\gamma^\mu\psi(x) = m\psi(x)$

Interactions w/ quantum foam: $g > 2$

$a_\mu = \frac{g-2}{2}$

Muon anomaly

Introduction

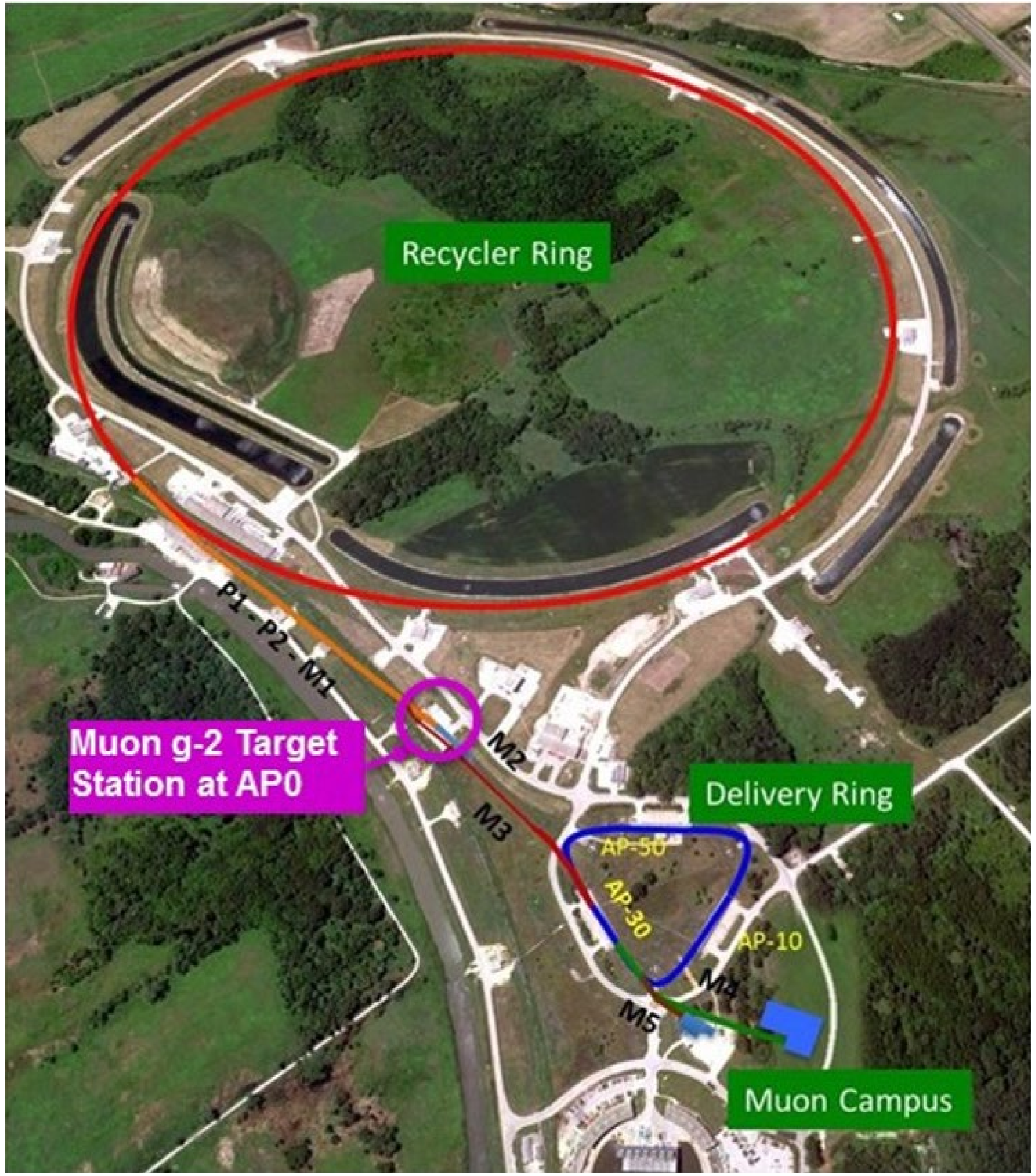

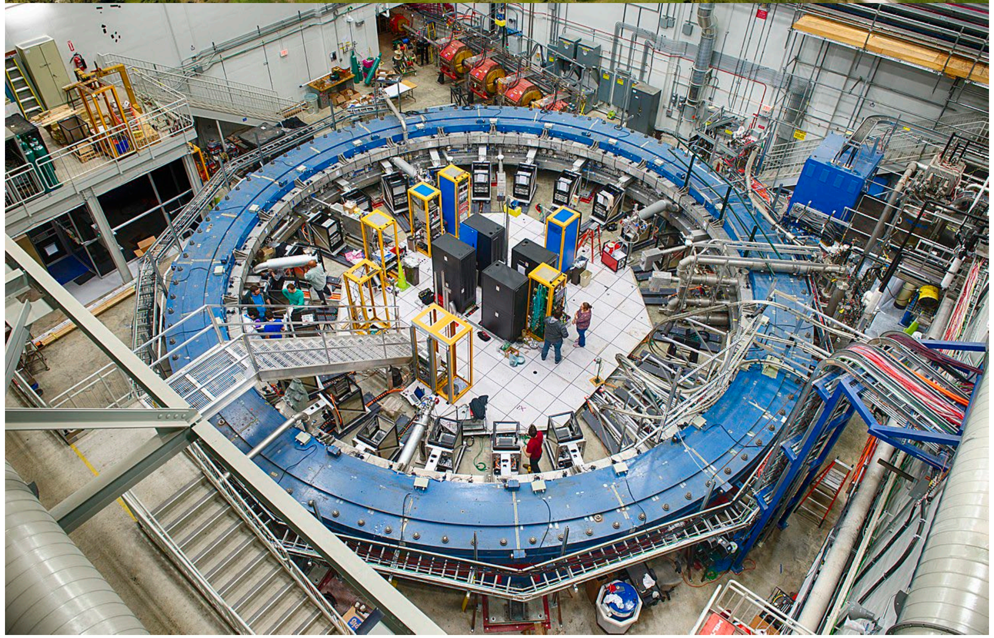

The Muon g-2 Storage Ring

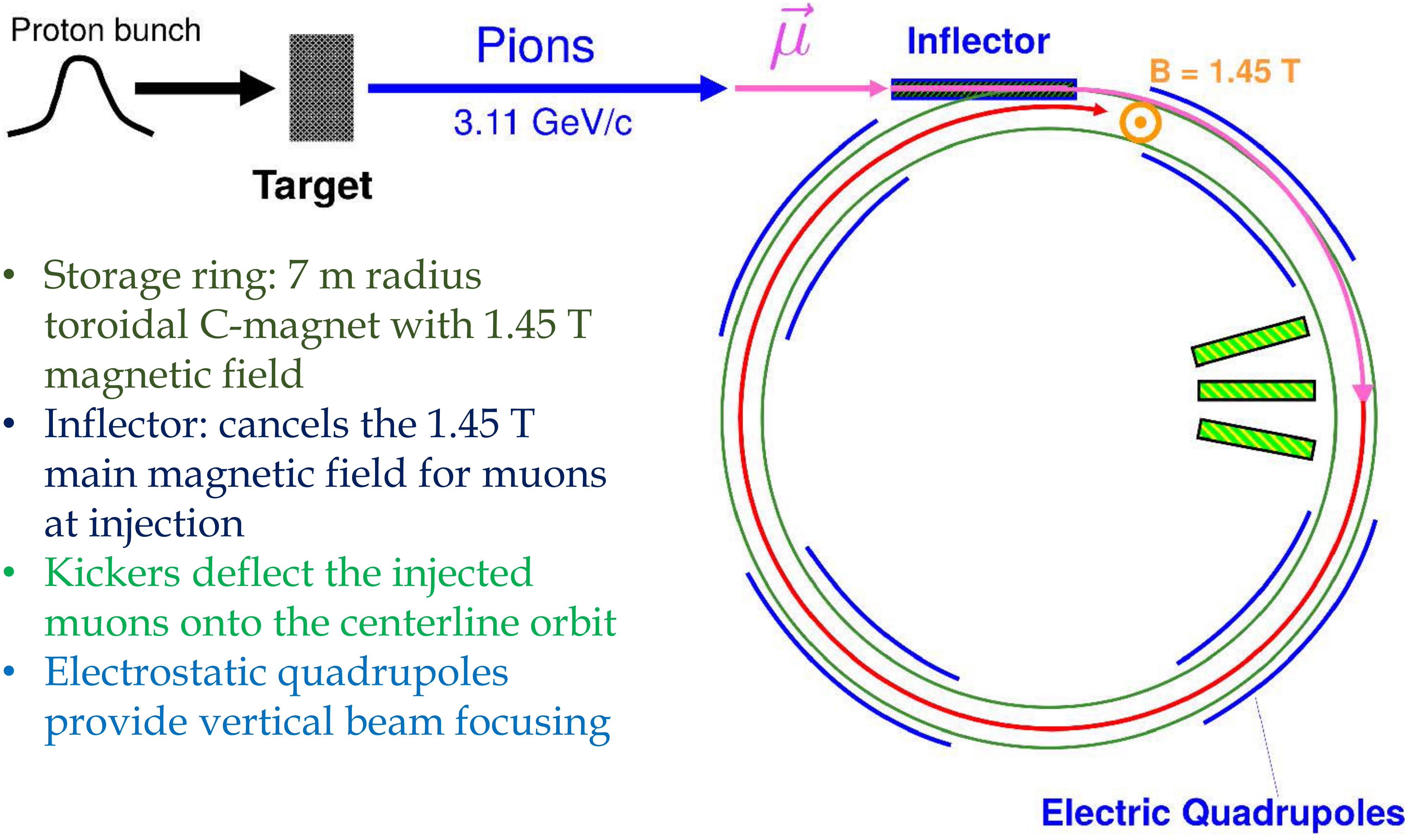

- Storage ring: 7 m radius toroidal C-magnet with 1.45 T magnetic field
- Inflector: cancels the 1.45 T main magnetic field for muons at injection
- Kickers deflect the injected muons onto the centerline orbit
- Electrostatic quadrupoles provide vertical beam focusing

a_μ Measurement Using a Storage Ring

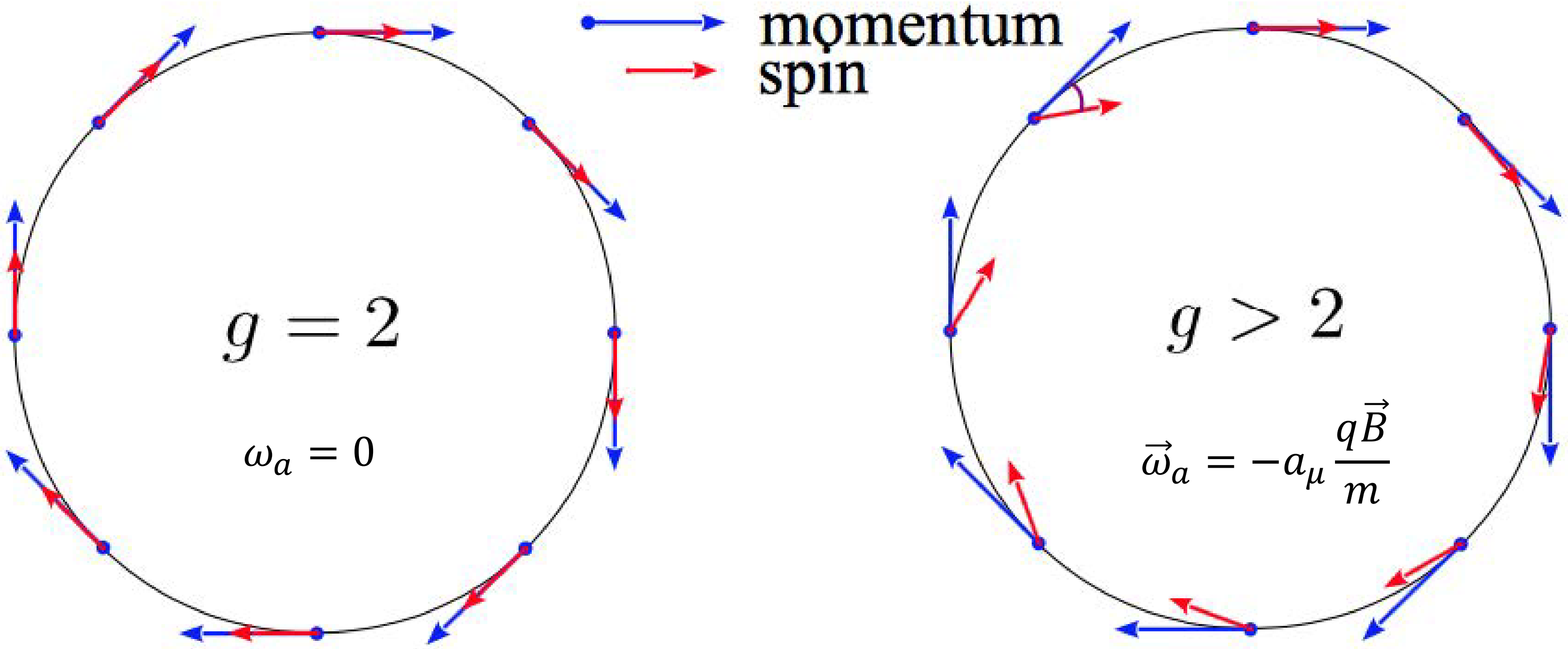

If g=2, the angle between the magnetic moment and the momentum does not change.
If g>2, the angle between the magnetic moment and the momentum changes linearly.

Result from Runs 1-3

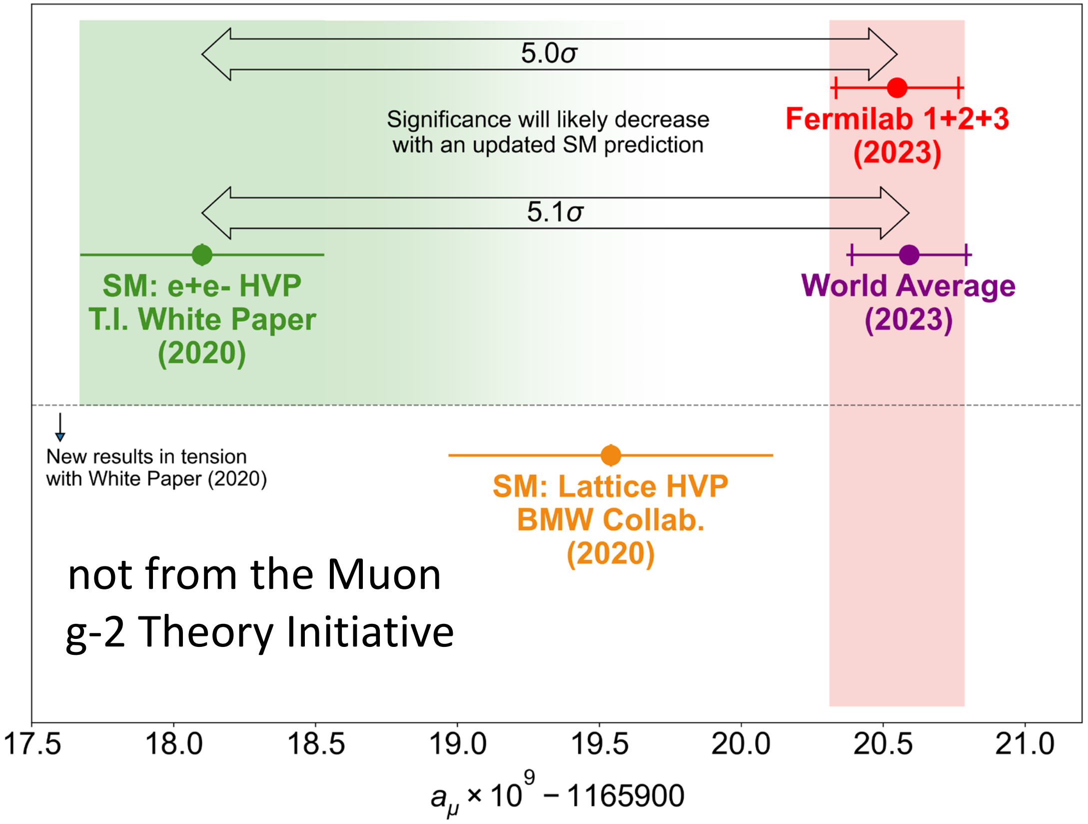

Quantity	Correction [ppb]	Uncertainty [ppb]
ω_a^m (statistical)	–	201
ω_a^m (systematic)	–	25
C_e	451	32
C_p	170	10
C_{pa}	-27	13
C_{dd}	-15	17
C_{ml}	0	3
$f_{\text{calib}} \langle \omega'_p(\vec{r}) \times M(\vec{r}) \rangle$	–	46
B_k	-21	13
B_q	-21	20
$\mu'_p(34.7°)/\mu_e$	–	11
m_μ/m_e	–	22
$g_e/2$	–	0
Total systematic	–	70
Total external parameters	–	25
Totals	622	215

a_μ (FNAL) = 0.00 116 592 055(24) [203 ppb]

a_μ (Exp) = 0.00 116 592 059(22) [190 ppb]

a_μ (Th) = 0.00 116 591 810(43) [370 ppb] (Review by Keshavarzi, 2022)

$$a_\mu = \frac{\omega_a}{\tilde{\omega}'_p(T_r)} \frac{\mu'_p(T_r)}{\mu_e(H)} \frac{\mu_e(H)}{\mu_e} \frac{m_\mu}{m_e} \frac{g_e}{2}$$

g_e = -2.002 319 304 361 82(52) (0.00026 ppb)

m_μ/m_e = 206.768 2826(46) (22 ppb)

μ_e/μ_p = -658.210 6866(20) (3.0 ppb)

Measurement by the Experiment

$$\mathcal{R}'_\mu = \frac{\omega_a}{\tilde{\omega}'_p(T_r)} = \frac{f_{\text{clock}}\ \omega_a^m\,(1 + C_e + C_p + C_{ml} + C_{pa})}{f_{\text{calib}}\ \langle \omega_p(x,y,\phi) \times M(x,y,\phi)\rangle (1 + B_k + B_q)}$$

- Unblinding conversion factor: f_{clock}
- Measured $g-2$ frequency: ω_a^m
- Corrections from the beam dynamics systematic effects: $C_e + C_p + C_{ml} + C_{pa}$
- NMR probe calibration factor: f_{calib}
- Magnetic field weighted over the muon distribution and azimuthally averaged: $\langle \omega_p(x,y,\phi) \times M(x,y,\phi)\rangle$
- Corrections from the transient magnetic field: $B_k + B_q$

E-field and Pitch Correction

E-field Correction

- Radial electric field

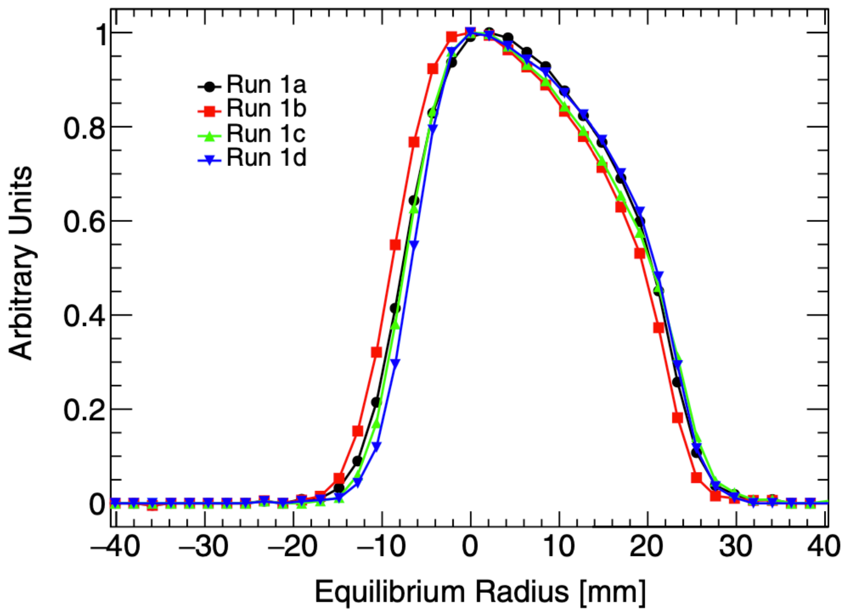

$$C_e = \frac{n_0 {\beta_0}^2}{1 - n_0} 2 \left\langle \left(\frac{dp}{p_0} \right)^2 \right\rangle = 451(32) \text{ ppb}$$

n_0: average quadrupole field index

$\beta_0 = p_0 / \sqrt{m^2 c^2 + {p_0}^2}$

Pitch Correction

- Average pitch angle relative to $B_y \overrightarrow{e_y}$

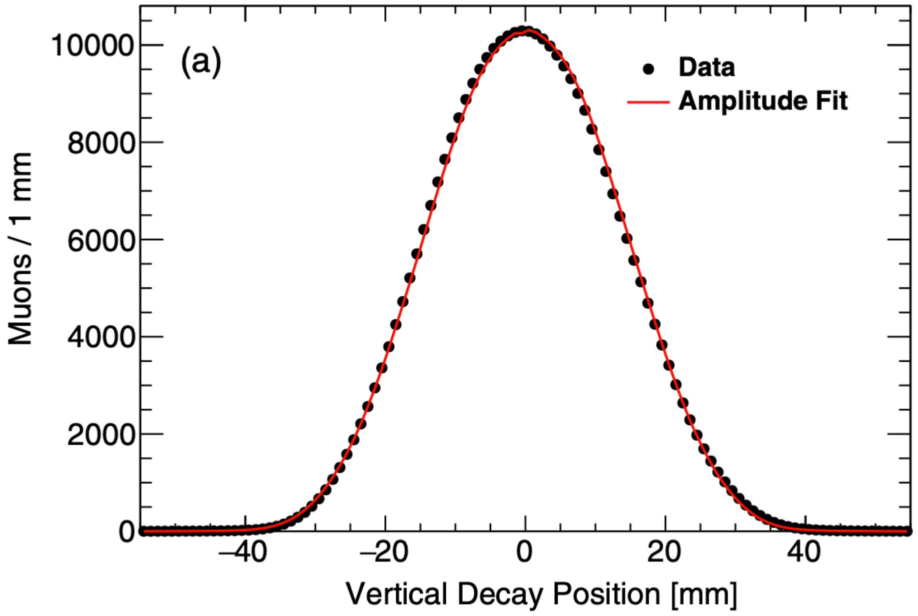

$$C_p = \frac{n_0}{2{\rho_0}^2} \langle y^2 \rangle = 170(10) \text{ ppb}$$

ρ_0: reference radius

Muon Loss Correction

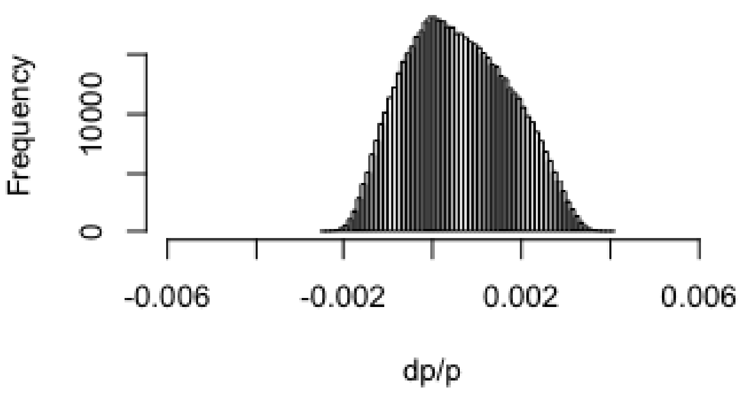

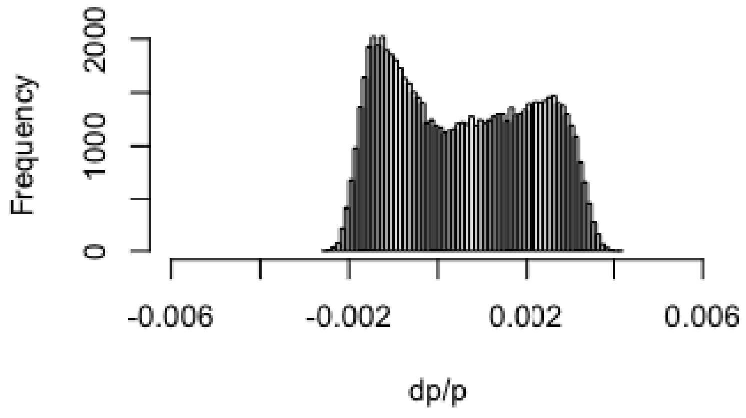

$$\frac{d\varphi_0}{dt} = \frac{d\varphi_0}{d\langle p\rangle}\frac{d\langle p\rangle}{dt}$$

$$C_{\mathrm{ml}} = 0(3)\ \mathrm{ppb}$$

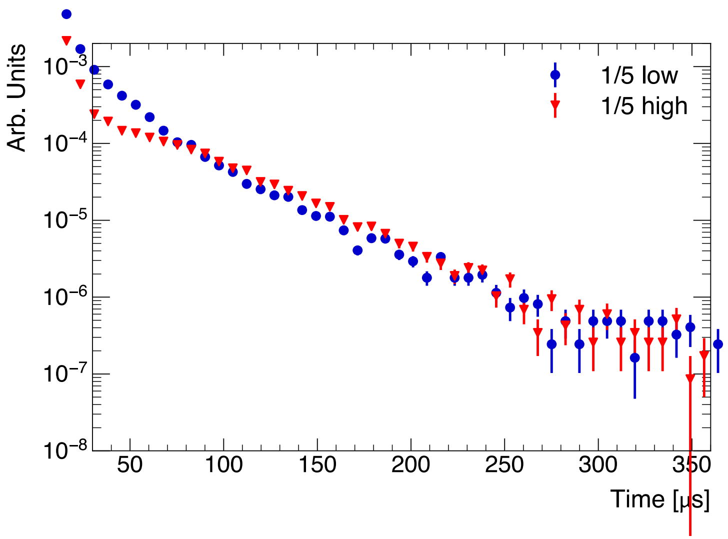

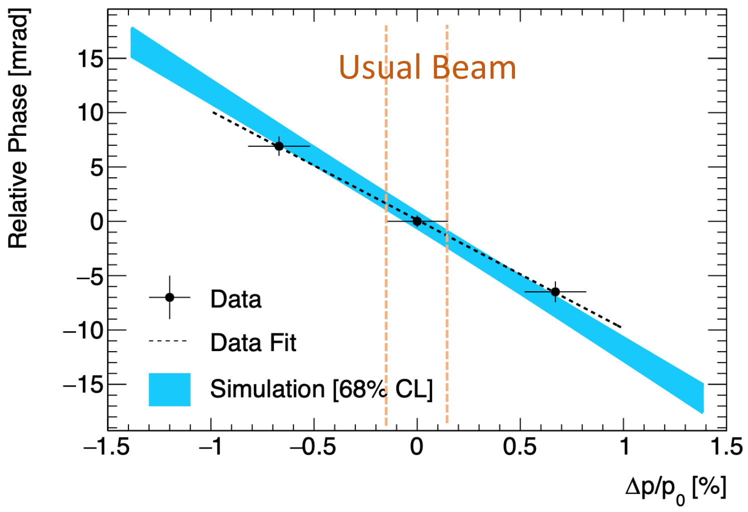

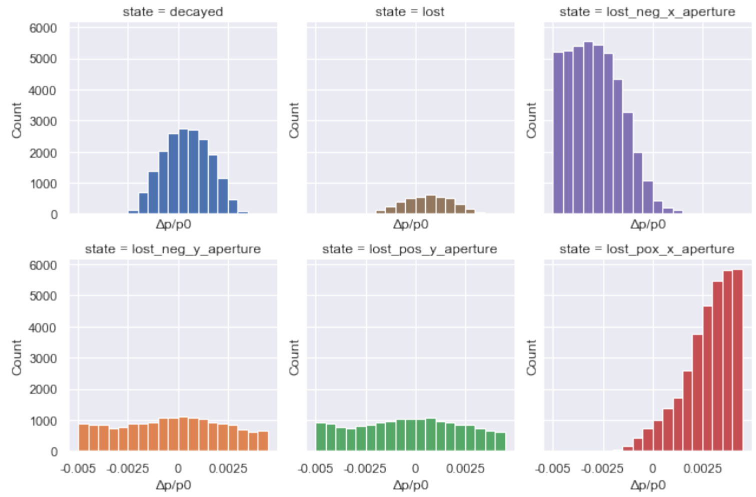

Phase Acceptance Correction

Phase Acceptance Correction

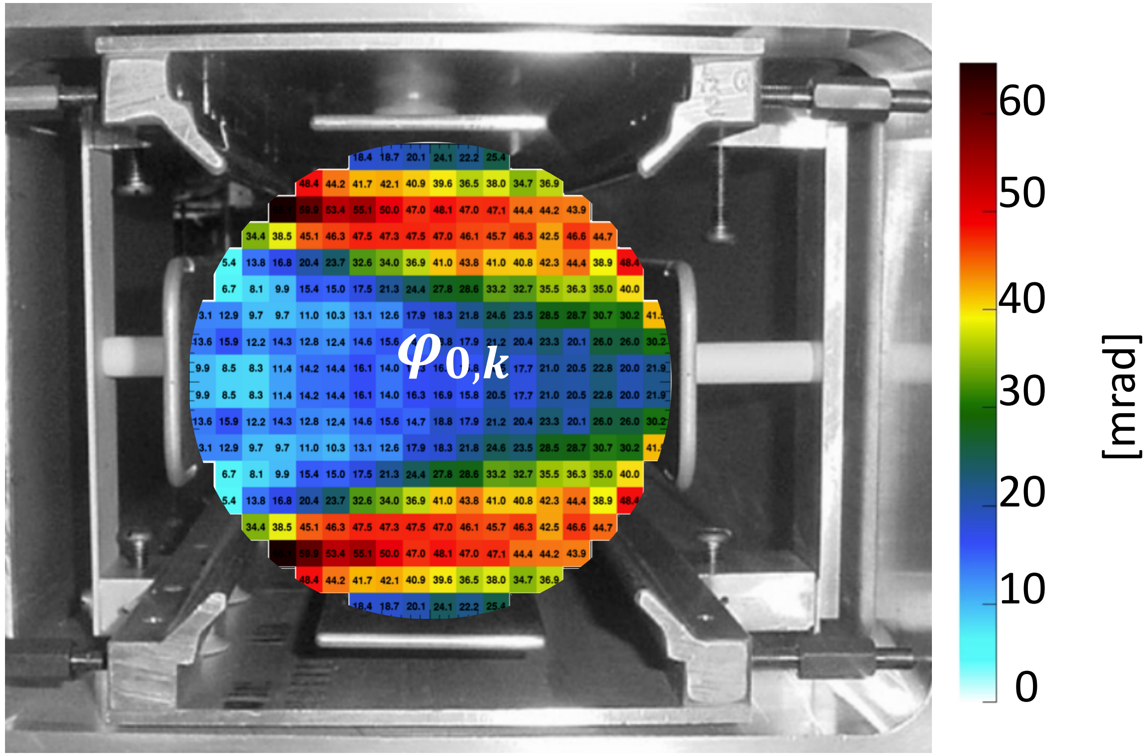

$C_{pa} = -27(13)$ ppb

A non-trivial **correlation** between the **muon decay radial and vertical position** within the 9-cm-diameter storage volume **and** the detector acceptance vs. the spin orientation of the muon at the time of its decay

- Formerly a high-priority topic
- A 10 billion event simulation-based study was performed (Kim Siang Khaw, …, Eremey Valetov, …)
- Custom NERSC simulation workflow

Muon Campus and Storage Ring Simulation Codes

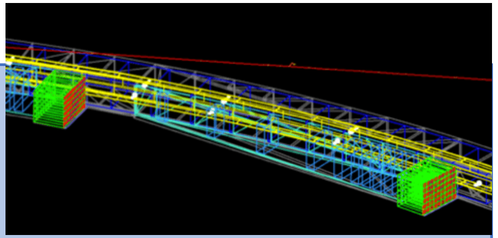

gm2ringsim
- Custom simulation tool
- Based on **geant4**
- **FHiCL** configuration language
- **art** event processing
- **Extensive custom source code including geometry, storage ring modules, etc.**

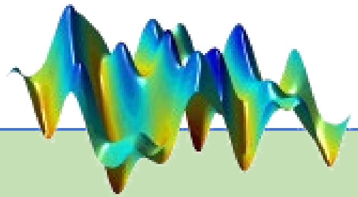

COSY INFINITY
- The most accurate storage ring model
- High-order DA transfer maps
- Accurate, Maxwellian fringe fields
- Symplectic tracking
- Electrostatic quadrupole multipole expansion up to order 24
- **Heavy duty long-term tracking**

BMAD
- Similar to **MAD**, with substantial expansions
- The storage ring and the Muon Campus
- **Custom pion decay code**

G4beamline
- Model of the Muon Campus beamlines and target station
- Based on **geant4**
- **Comprehensive physics and geometry modeling, compared to BMAD**
- Overlapping coordinate system limitation in ring lattice modeling

MARS
- A highly accurate Monte Carlo code for modeling of radiation transport and interaction with matter
- Used for the Muon *g*-2 **target station**

High-Performance Tracking for Large Phase Space Distributions

2×10^8 muon simulation for Fourier analyses studies

Conventional

gm2ringsim

2×10^8 muons: 560 days with 1e3 CPUs

Hybrid

gm2ring-sim → COSY INFINITY

Injection

~70 to 130 turns
~5 to 130 μs

~1700 turns
~250 μs

Scraping using CAD geometry

Efficient long-term tracking

- Less than 1 day

Nonlinear Transfer Map and Differential Algebras

Linear transfer map

$$\begin{pmatrix} x \\ a \\ y \\ b \\ l \\ \delta \end{pmatrix}_{\mathrm{f}} =_1 \begin{pmatrix} M_{xx} & \cdots & M_{x\delta} \\ \vdots & \ddots & \vdots \\ M_{\delta x} & \cdots & M_{\delta\delta} \end{pmatrix} \begin{pmatrix} x \\ a \\ y \\ b \\ l \\ \delta \end{pmatrix}_{\mathrm{i}}$$

Nonlinear transfer map

$$z_i = \sum_{j\geq 1} \sum_{j_1+\cdots+j_n=j} \frac{1}{j_1!\cdots j_n!} \boxed{\left(z_i | z_1^{j_1} \cdots z_n^{j_n}\right)} z_1^{j_1} \cdots z_n^{j_n}$$

Aberrations

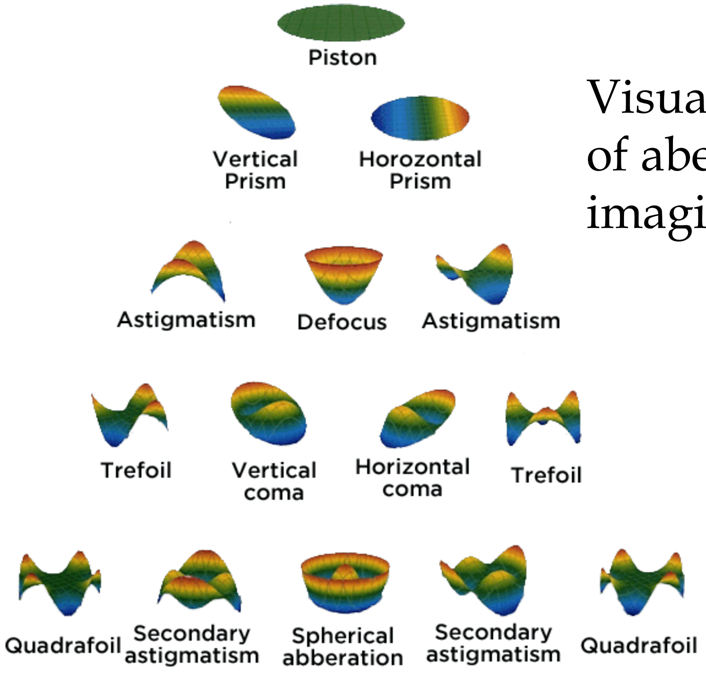

Visual classification of aberrations in imaging

Differential Algebras (DA): algebras operating on objects equivalent to truncated Taylor expansions

- Include integration and differentiation operators
- *COSY INFINITY* has highly optimised DA data types

Analytical Calculation of Aberrations, Tunes, and Chromaticities

1. Analytic aberrations formula:
- Order-by-order perturbation method
- Use transfer map methods:

$$\frac{d}{ds}\vec{r} = M(s)\vec{r} + \sum_{j=2}^{+\infty} N_j(\vec{r}, s)$$

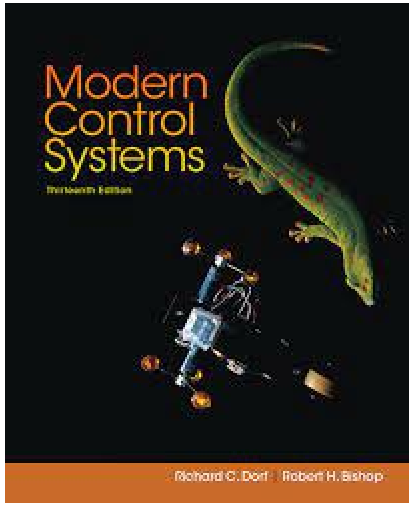

One beamline element:
partwise $M(s) = \text{const}$:
$\vec{r}_{\mathrm{f}} =_1 \exp(Ms)\vec{r}_{\mathrm{i}}$

2. Obtain the transfer map for one turn around the storage ring by composition

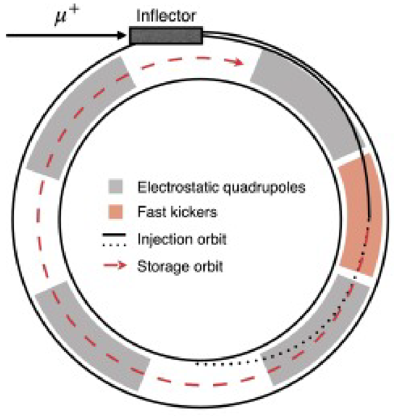

(a)

3. Calculate the tunes:

$$Q_{x,y} = \frac{1}{2\pi}\arccos\left(\frac{\mathrm{tr}\left(M_{x,y}\right)}{2}\right)$$

4. Calculate the chromaticities:
(Long formula in terms of first and second–order transfer map elements)

Muon g-2 Storage Ring Chromaticity

Notes on Chromaticity – Overview

G Minus 2 Experiment Document 29571

Eremey Valetov, Martin Berz, and Kyoko Makino

November 15, 2023

Depar

1 Introduction

We derived analytic formu
high voltage electrostatic
electrostatic quadrupole [7
results. We used the follow

1. **"Modular ring"** (DI

Horizontal Aberrations of the Muon $g-2$ High Voltage Electrostatic Quadrupole With Superimposed Dipole Field

G Minus 2 Experiment Document 29657

Eremey Valetov, Martin Berz, and Kyoko Makino

December 4, 2023

Department of Physics and Astronomy, Michigan State University

Cont

1 **Intr**
2 **Equ**
3 **Ord**
4 **Cor**
4.1
4.2

Chromaticity of the Muon $g-2$ Storage Ring

G Minus 2 Experiment Document 29717

Eremey Valetov, Martin Berz, and Kyoko Makino

December 10, 2023

Contents

Comments on E989 Note 167

G Minus 2 Experiment Document 2XXXX

Eremey Valetov, Martin Berz, and Kyoko Makino

December 11, 2023

Department of Physics and Astronomy, Michigan State University

Contents

For the second order horizontal DIQ aberrations, we obtained

$$(x|xx) = -2h^3\vartheta^{-2}\left(1-3n+(1-2n)\cos(\vartheta s)\right)\sin^2(\vartheta s/2)\,, \tag{13a}$$

$$(x|xa) = h^3\vartheta^{-3}\left(n+(1-2n)\cos(\vartheta s)\right)\sin(\vartheta s)\,, \tag{13b}$$

$$(x|aa) = 2h^3\vartheta^{-4}\left(n+(1-2n)\cos(\vartheta s)\right)\sin^2(\vartheta s/2)\,, \tag{13c}$$

$$\begin{aligned}(x|x\delta_K) = {}& h^4\vartheta^{-4}\gamma_0^{-1}(1+\gamma_0)^{-1}\cdot\\ &\cdot\sin(\vartheta s/2s)\left(\vartheta ns\left(n-1+(2+n)\gamma_0^2\right)\cos(\vartheta s/2)-\right.\\ &\left.-2\gamma_0^2\left(3n-1+(2n-1)\cos(\vartheta s)\right)\sin(\vartheta s/2)\right)\,,\end{aligned} \tag{13d}$$

$$\begin{aligned}(x|a\delta_K) = {}& \frac{1}{2}h^4\vartheta^{-5}\gamma_0^{-1}(1+\gamma_0)^{-1}\cdot\\ &\cdot\left(n\sin(\vartheta s)\left(n-1+(2-n)\gamma_0^2\right)-\right.\\ &\left.-\cos(\vartheta s)\left(\vartheta ns\left(n-1+(n+2)\gamma_0^2\right)+2(1-2n)\gamma_0^2\sin(\vartheta s)\right)\right)\,,\end{aligned} \tag{13e}$$

$$\begin{aligned}(x|\delta_K\delta_K) = {}& h^5\vartheta^{-7}(1+\gamma_0)^{-2}\cdot\\ &\cdot\sin(\vartheta s/2)\left(2h^2(n-1)ns\left(n-1+(n+2)\gamma_0^2\right)\cos(\vartheta s/2)+\right.\\ &\left.+2\vartheta\left(n^2-1+(6n-1)\gamma_0^2+(2n-1)\gamma_0^2\cos(\vartheta s)\right)\sin(\vartheta s/2)\right)\,,\end{aligned} \tag{13f}$$

$$(a|xx) = h^3\vartheta^{-1}n\left(\sin(\vartheta s)+\sin(2\vartheta s)\right)\,, \tag{13g}$$

$$(a|xa) = h^3\vartheta^{-2}n\left(\cos(\vartheta s)-\cos(2\vartheta s)\right)\,, \tag{13h}$$

$$(a|aa) = h^3\vartheta^{-3}\left(3n-1-2n\cos(\vartheta s)\right)\sin(\vartheta s)\,, \tag{13i}$$

$$\begin{aligned}(a|x\delta_K) = {}& \frac{1}{2}h^4\vartheta^{-3}n\gamma_0^{-1}(1+\gamma_0)^{-1}\cdot\\ &\cdot\left(\vartheta s\left(\gamma_0^2(n+2)+n-1\right)\cos(\vartheta s)+\right.\\ &\left.+\sin(\vartheta s)\left(n-1-4\gamma_0^2\cos(\vartheta s)-\gamma_0^2(n-2)\right)\right)\,,\end{aligned} \tag{13j}$$

$$\begin{aligned}(a|a\delta_K) = {}& \frac{1}{2}h^4\vartheta^{-4}n\gamma_0^{-1}(1+\gamma_0)^{-1}\cdot\\ &\cdot\left(\vartheta s\left(\gamma_0^2(n+2)+n-1\right)\sin(\vartheta s)-2\gamma_0^2\cos(\vartheta s)+2\gamma_0^2\cos(2\vartheta s)\right)\,,\end{aligned} \tag{13k}$$

$$\begin{aligned}(a|\delta_K\delta_K) = {}& h^5\vartheta^{-5}(1+\gamma_0)^{-2}\cdot\\ &\left(\sin(\vartheta s)\left(2\gamma_0^2n\cos(\vartheta s)+\gamma_0^2n^2+n-1\right)-\right.\\ &\left.-\vartheta ns\left(\gamma_0^2(n+2)+n-1\right)\cos(\vartheta s)\right)\,,\end{aligned} \tag{13l}$$

and $(\delta_K|z_{j_1}z_{j_2})=0$ for all j_1 and j_2.

Excellent agreement between analytic formulas and *COSY INFINITY*

Model DIEQ

Method	$\xi_x^{(p)}$
Valetov, analytic	−0.1423355243040865
COSY INFINITY	−0.1423355242929523

Model DIQ360

Method	$\xi_x^{(p)}$
Valetov, analytic	−0.1479827303263903 4
COSY INFINITY	−0.1479827303376410

Model DIEQ_ON

Method	$\xi_x^{(p)}$
Valetov, analytic	−0.1600503684164580 3
COSY INFINITY	−0.1600503684287856

Excellent agreement between analytic formulas and ***COSY INFINITY***

Model DIEQ

Method	$\xi_x^{(p)}$
Valetov, analytic	-0.1423355243040865
COSY INFINITY	-0.1423355242929523

Model DIQ360

Method	$\xi_x^{(p)}$
Valetov, analytic	$-0.1479827303263903$4
COSY INFINITY	-0.1479827303376410

Model DIEQ_ON

Method	$\xi_x^{(p)}$
Valetov, analytic	$-0.1600503684164580$3
COSY INFINITY	-0.1600503684287856

Amplitude Dependent Tune Shifts

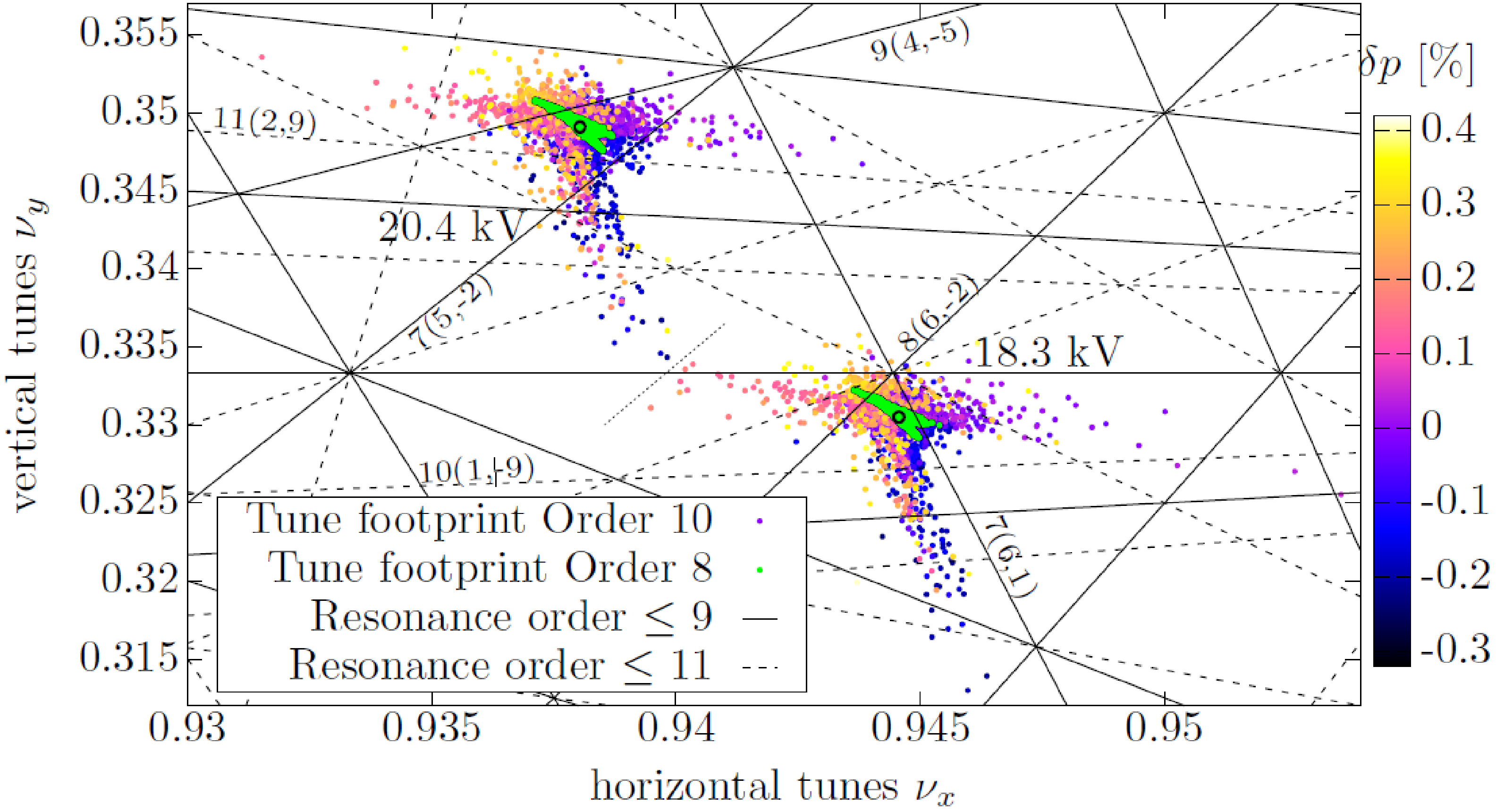

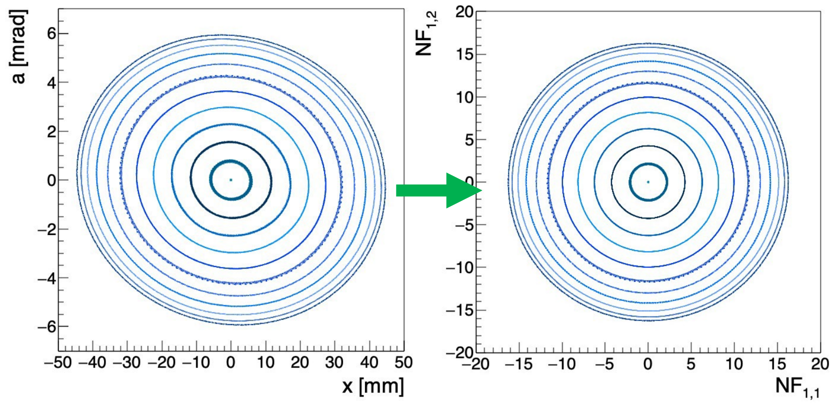

- ***COSY INFINITY*** provides automatic conversion to nonlinear normal form coordinates
- Normal forms: dynamics described by constant angle advancement, which is dependent on the amplitude and parameters in a straightforward way

A. Weisskopf, D. Tarazona, M. Berz, Int. Journal of Modern Physics A, 34, 36 (2019) 1942011. DOI: 10.1142/S0217751X19420119

Symplectic Tracking

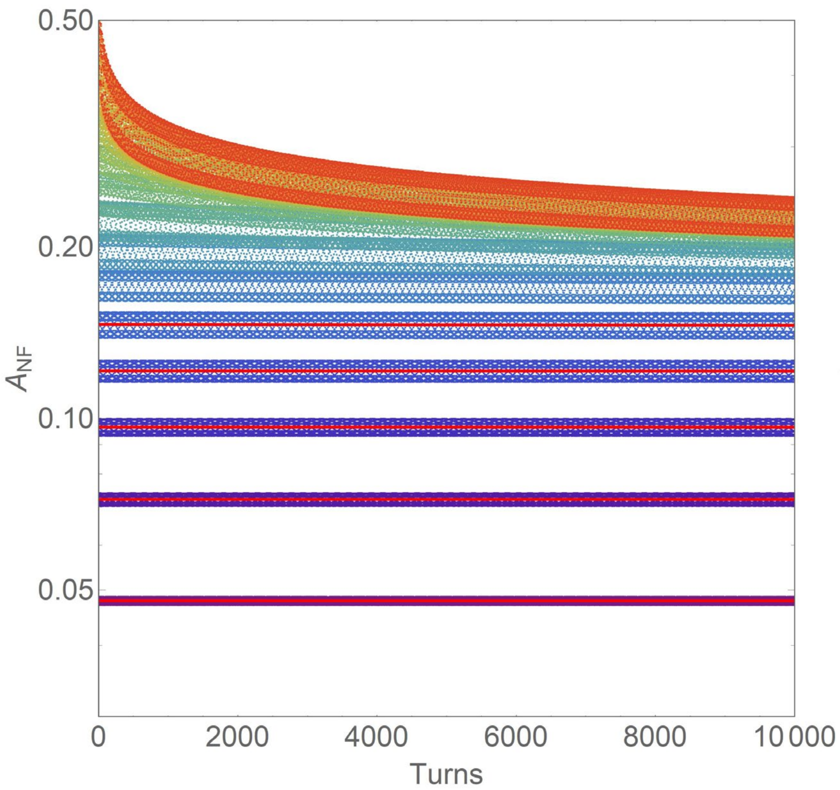

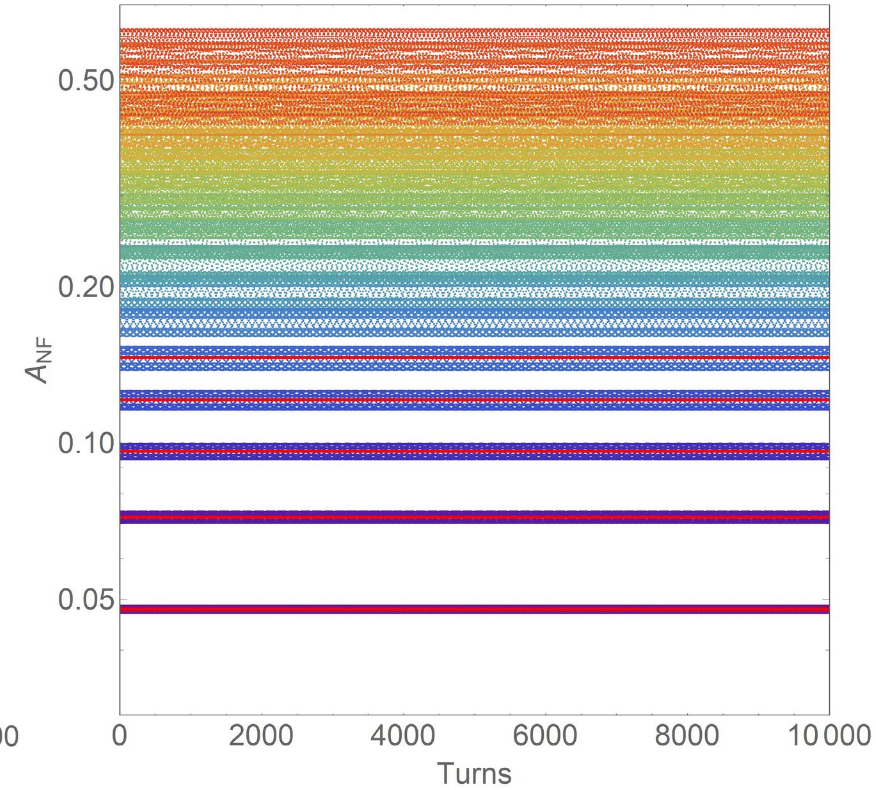

Normal form horizontal transverse amplitude vs. the number of turns for a test case of a cell defined as the 45° electrostatic deflector of radius 1 m. A set of rays is tracked without symplectification (left) and with symplectification (right).

E. Valetov, M. Berz, Advances in Imaging and Electron Physics, 213, 6 (2020).
DOI: 10.1016/bs.aiep.2019.11.007

COSY INFINITY ensures preservation of phase space volume in simulation of the Muon g-2 storage ring using symplectic tracking

Symplectic tracking for the full Hamiltonian without approximations is generally one of the most challenging topics in beam dynamics simulations

Conformal Mapping Methods

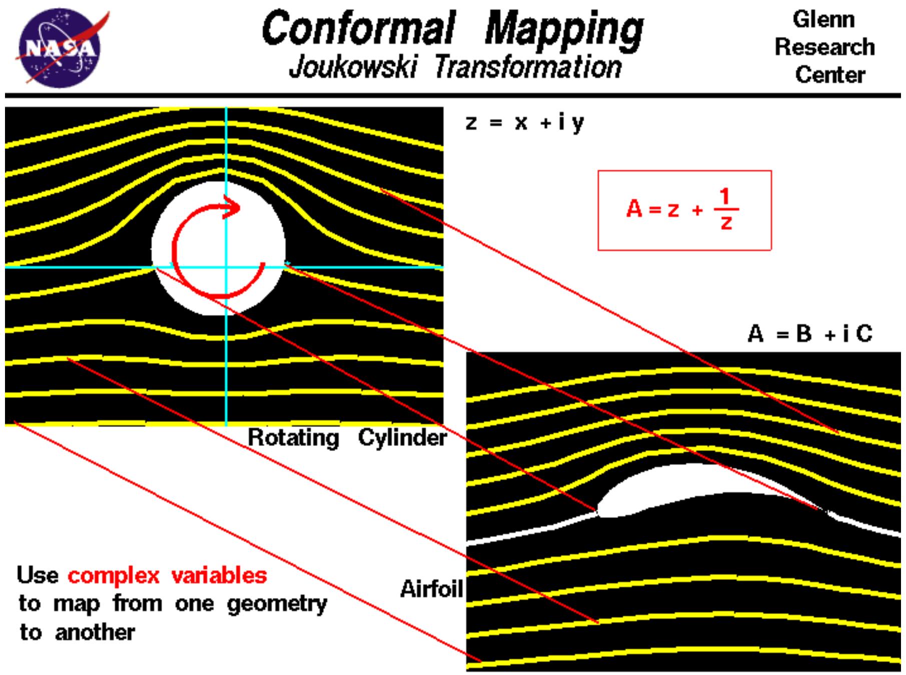

Image credit: NASA's Glenn Research Center.

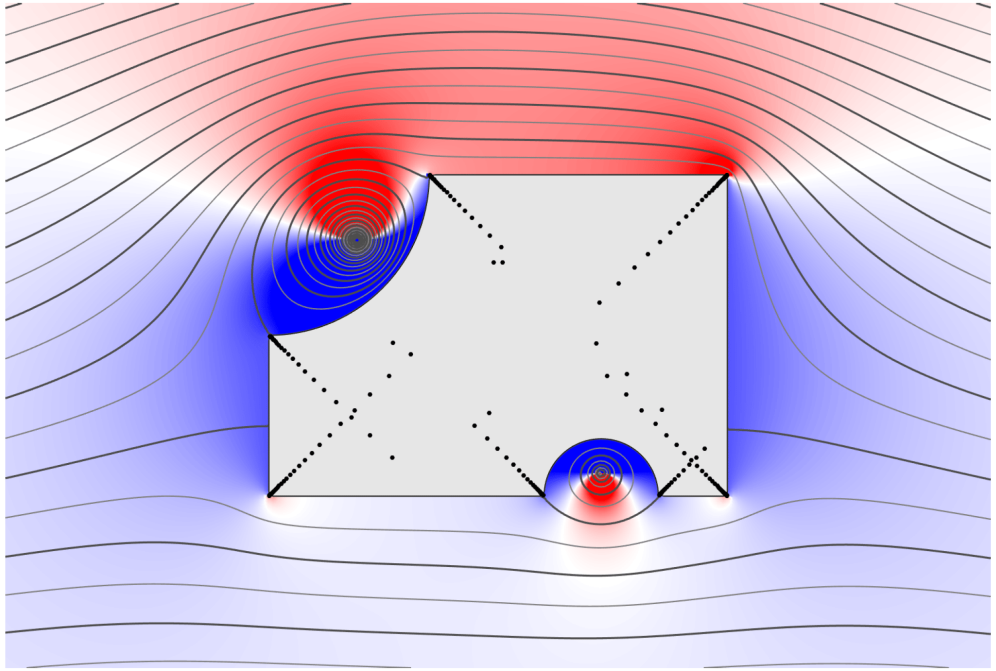

Image credit: Peter Baddoo.

Advantages of conformal mappings for field calculations

Fully Maxwellian

Possibility or rapid recalculations (e.g., for voltage asymmetries or plate offsets)

Multipole Expansion of the Quadrupole Potential

(Up to order 24)

Field dominated by quadrupole moment

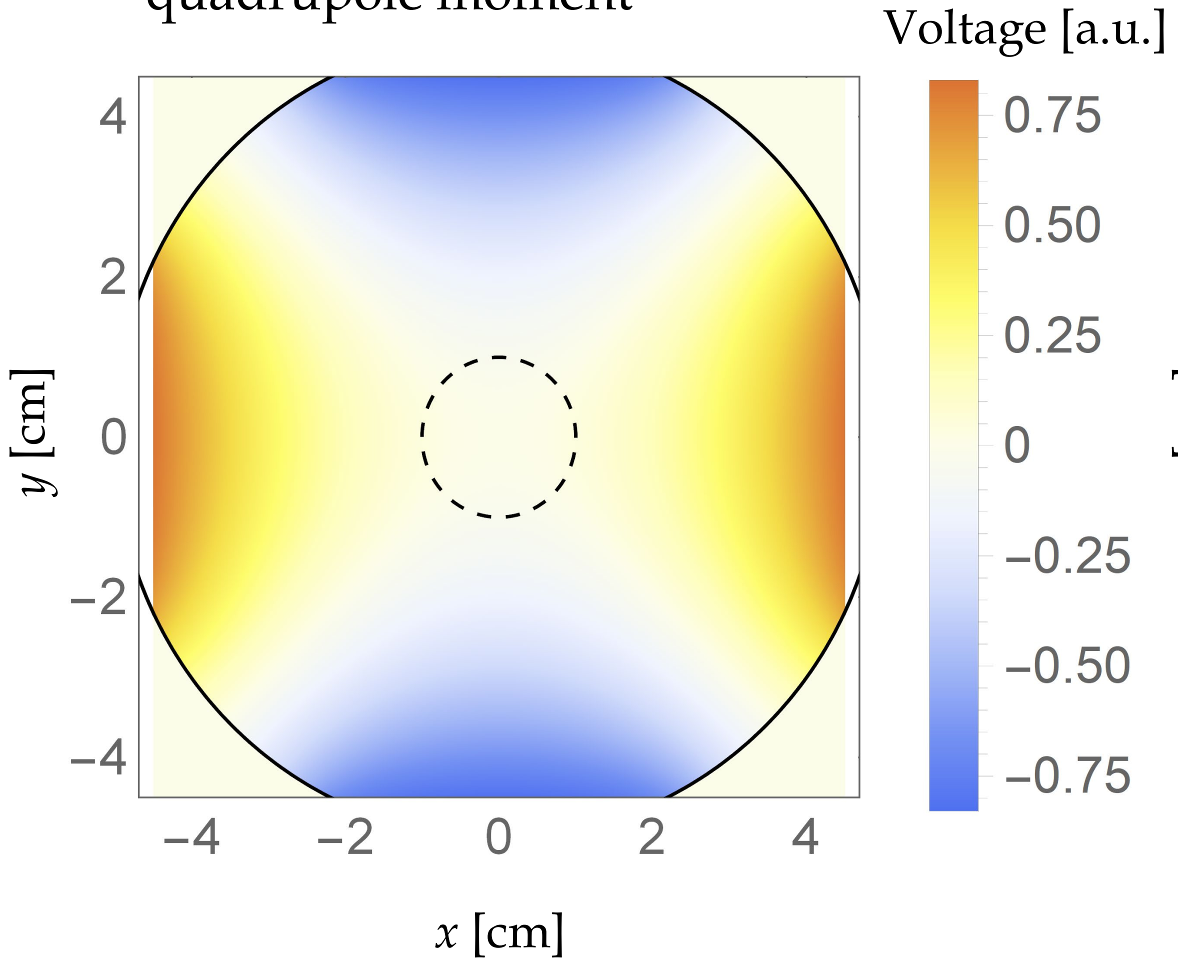

Higher order multipoles after quadrupole subtraction

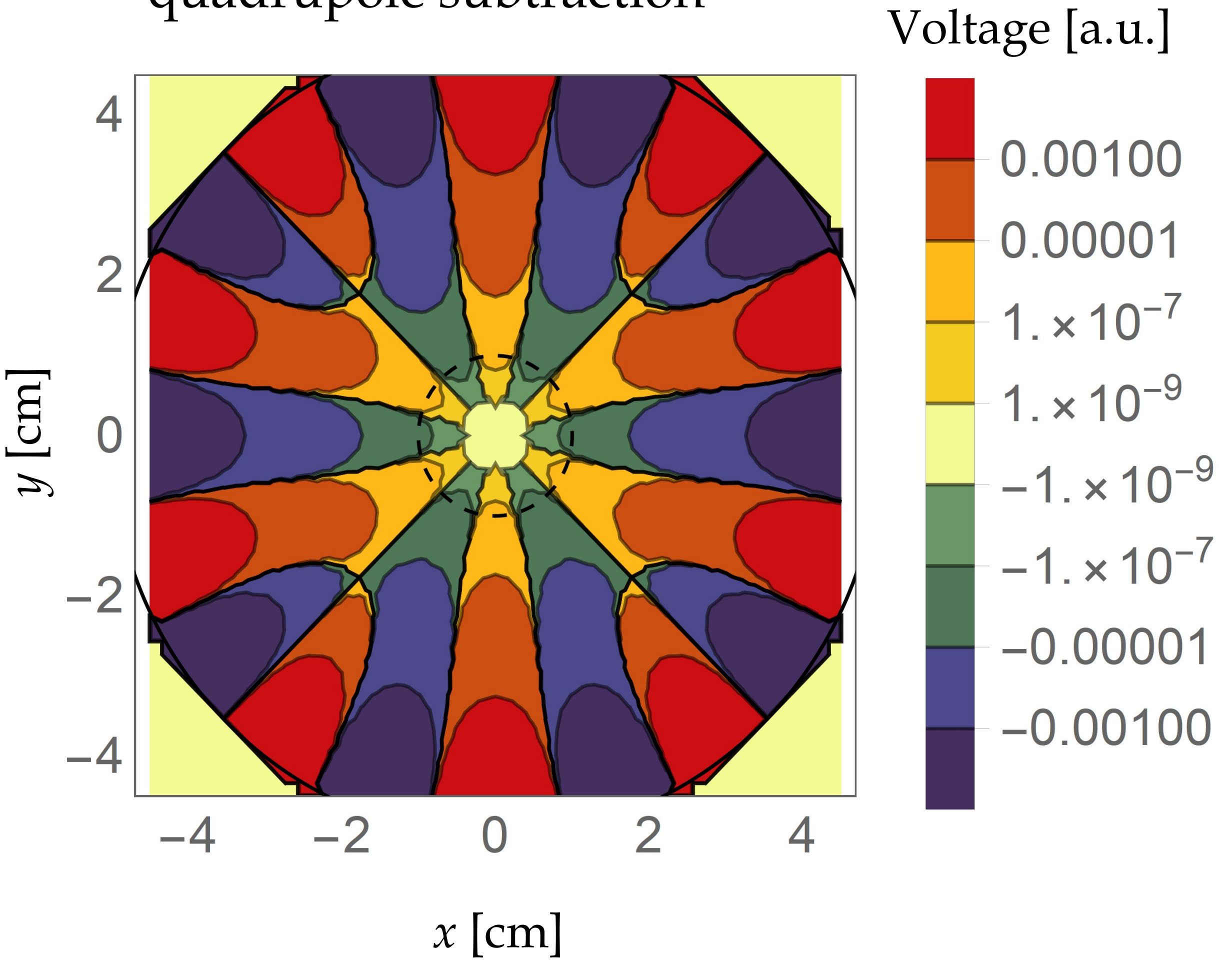

Data Acquisition as a Multiple of BNL Data

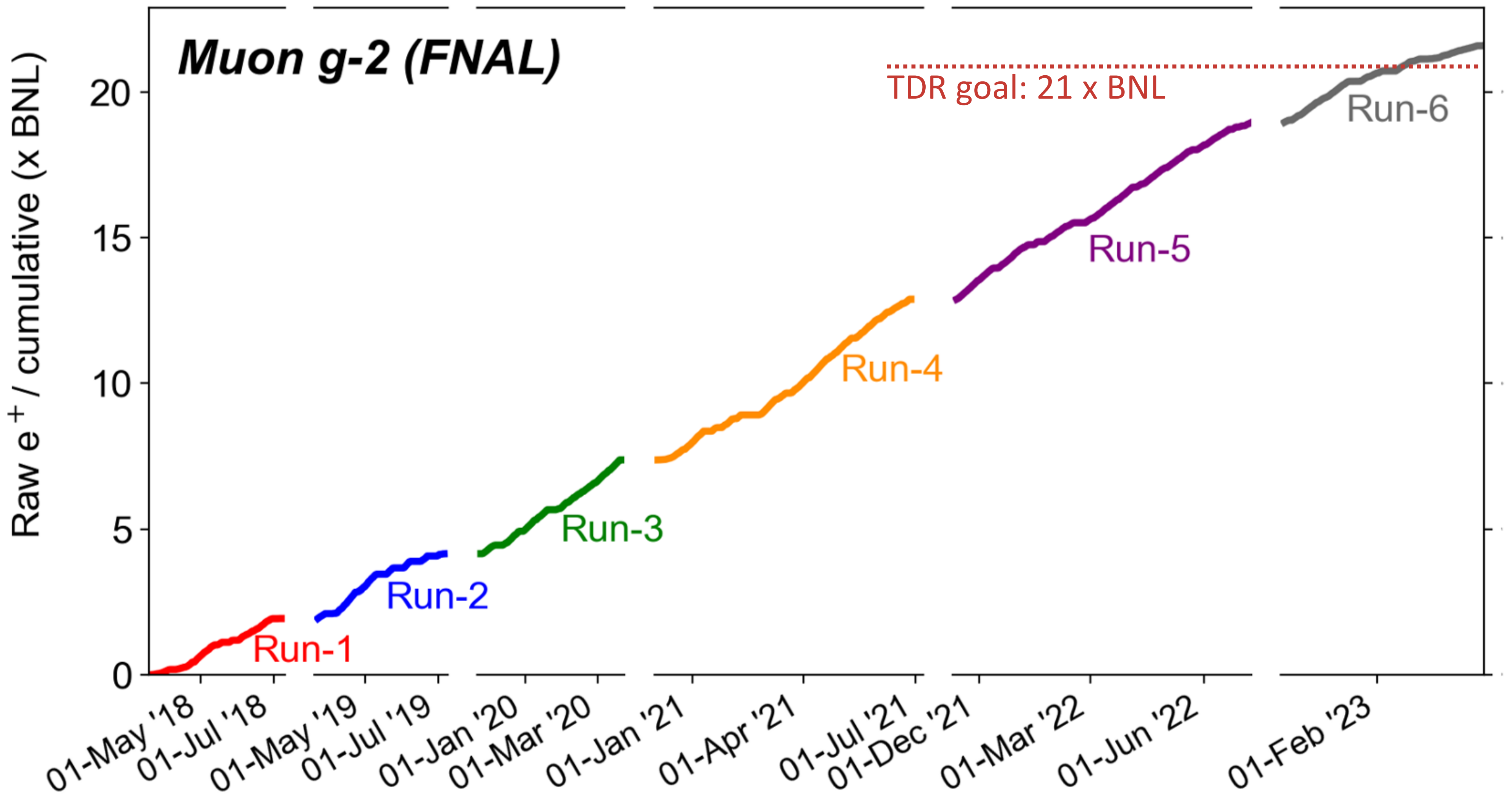

Conclusion

- Results based on Runs 2-3 were published in August 2023
- The experiment has completed its final Run 6 in July 2023
    - 21x more raw data than the Muon g-2 Experiment at BNL
    - Improving systematics:
        - Magnet temperature control
        - Magnetic field noise control
        - Analysis improvements (pileup reconstruction)
    - Achieved the TDR goal of 70 ppb systematic error
- Results from runs 4-6 planned to be released in 2025
    - We derived chromaticity formulas to support the analyses
- New theory results expected in 2025

Conclusion

USA
- Boston
- Cornell
- Illinois
- James Madison
- Kentucky
- Massachusetts
- Michigan
- Michigan State
- Mississippi
- North Central
- Northern Illinois
- Regis
- Virginia
- Washington

USA National Labs
- Argonne
- Brookhaven
- Fermilab

182 collaborators
33 Institutions
7 countries

China
- Shanghai Jiao Tong

Germany
- Dresden
- Mainz

Italy
- Frascati
- Molise
- Naples
- Pisa
- Roma Tor Vergata
- Trieste
- Udine

Korea
- CAPP/IBS
- KAIST

Russia
- Budker/Novosibirsk
- JINR Dubna

United Kingdom
- Lancaster/Cockcroft
- Liverpool
- Manchester
- University College London

Collaboration meeting at University of Liverpool, July 2023
Photo credit: McCoy Wynne

U.S. DEPARTMENT OF ENERGY | Office of Science

- The Center for Beam Theory and Dynamic Systems at Michigan State University acknowledges support from the U.S. Department of Energy, Office of Science, under Contracts No. DE-FG02-08ER41546 and DE-SC0018636.
- This document was prepared by the Muon g-2 collaboration using the resources of the Fermi National Accelerator Laboratory (Fermilab), a U.S. Department of Energy, Office of Science, HEP User Facility. Fermilab is managed by Fermi Research Alliance, LLC (FRA), acting under Contract No. DE-AC02-07CH11359.
- This research used resources of the National Energy Research Scientific Computing Center (NERSC), a U.S. Department of Energy Office of Science User Facility operated under Contract No. DE-AC02-05CH11231.
- This research was done using resources provided by the Open Science Grid, which is supported by the National Science Foundation award 1148698, and the U.S. Department of Energy's Office of Science.